Pressure Dependence of the CN($B^2\Sigma^+$–$X^2\Sigma^+$) Emission Spectra in an Ar Flowing Afterglow

Kazuhiro KANDA,* Kaoru SUZUKI,† Haruhiko ITO,†† Tamotsu KONDOW,††† and Kozo KUCHITSU††††
Department of Fundamental Science, College of Science and Engineering, Iwaki Meisei University, Iwaki, Fukushima 970
† Faculty of Foreign Studies, Tokoha Gakuen University, Shizuoka 420
†† Department of Chemistry, Nagaoka University of Technology, Nagaoka, Niigata 940-21
††† Department of Chemistry, School of Science, The University of Tokyo, Bunkyo-ku, Tokyo 113
†††† Department of Chemistry, Faculty of Science, Josai University, Sakado, Saitama 350-02
(Received April 25, 1994)

The CN($B^2\Sigma^+$–$X^2\Sigma^+$) emission spectrum produced in the reaction of Ar($^3P_2$) with BrCN was observed by the use of a flowing afterglow method at argon pressures ranging from 9 mTorr to 2 Torr (1 Torr=133.322 Pa). The pressure dependences of the intensity anomalies in the rotational lines due to the $B^2\Sigma^+\sim A^2\Pi_i$ and the $B^2\Sigma^+\sim{}^4\Sigma^+$ perturbations were measured by introducing collision-partner gases in the reaction region. These pressure dependences can be explained by the "doorway" model. On the other hand, the measured pressure dependence of the effective rotational temperature in the CN($B^2\Sigma^+$) state can also be reproduced by the collision-induced rotational relaxation model. The cross section for the rotational relaxation in the $A^2\Pi_i$ state was found to be smaller than those in the $B^2\Sigma^+$ and $^4\Sigma^+$ states. This finding is interpreted by the use of the dipole–induced dipole interaction model for the collision–induced rotational relaxation.

The CN($B^2\Sigma^+$–$X^2\Sigma^+$) emission spectra have been known to show a number of intensity anomalies, which are due to the local perturbation of the $B^2\Sigma^+$ state with other electronic states: $A^2\Pi_i$, $^4\Sigma^+$, $^4\Pi$, etc. These intensity anomalies have been reported to show strong pressure dependences by the collisional relaxations in the perturbing electronic state and the $B^2\Sigma^+$ state.[1—7] The intensity anomalies in the rotational lines at $N=7$ in the $B^2\Sigma^+$ ($v=14$)$\sim{}^4\Pi$ ($v=6$) perturbation were observed at an argon or helium pressure ranging between 9 mTorr and 2 Torr.[8] The observed intensities of the perturbed lines relative to that of the rotational band envelope increased with the ambient pressure in the low-pressure region, whereas they decreased with the pressure in the higher-pressure region. By the use of the "doorway" model, the increase in the low-pressure region was ascribed to the rotational relaxation in the $^4\Pi$ state, and the decrease in the higher-pressure region was explained by the collisional relaxation in the $B^2\Sigma^+$ state.

The purpose of this paper is to confirm our previous treatment of the pressure dependence of the CN ($B^2\Sigma^+$–$X^2\Sigma^+$) emission spectra and to draw general conclusions. In order to examine the applicability of the doorway model proposed in Ref. 8, a semiquantitative analysis based on this model is extended to an analysis of the pressure dependences of the intensity anomalies due to other local perturbations—the $B^2\Sigma^+$ ($v=0$)$\sim A^2\Pi_i$ ($v=10$)[9] and $B^2\Sigma^+$ ($v=11$)$\sim{}^4\Sigma^+$ perturbations observed at (v_B, N)=(0, 15) and (11, 20), respectively.[10] The intensities of the rotational lines at these perturbations are observed as a function of the argon pressure ranging from 9 mTorr to 2 Torr. In addition, the effective rotational temperature in the $B^2\Sigma^+$ ($v=15$) state is measured, since the pressure dependence of the rotational temperature is ascribable to the collisional relaxation in the unperturbed $B^2\Sigma^+$ state.

Experimental

The details of the flowing afterglow apparatus and the experimental procedure have been described in Ref. 8. Cyanogen bromide (Nacalai, purity 90%) was used after degassing. The CN($B^2\Sigma^+$–$X^2\Sigma^+$) emission was observed by a 1-m monochromator with the slit widths of 10 μm×20 mm (spectral resolution: 0.1 Å FWHM). The image of the entrance slit of the monochromator was set at a point just downstream of the sample injection nozzle. The collision partner, Ar, was introduced through an orifice on another flange to the reaction region in the flow tube. The pressure of rare gas in the reaction zone was monitored by a Pirani gauge, which was calibrated with a capacitance manometer (MKS Baratron).

Results and Discussion

Pressure Dependence of the Effective Rotational Temperature. The rotational temperature of the CN($B^2\Sigma^+$–$X^2\Sigma^+$) 15–15 band was observed as a function of the argon pressure ranging from 9 mTorr to 2 Torr. The $B^2\Sigma^+$ ($v=15$) state is one of the vibrational bands which are most weakly perturbed by the other electronic states. In addition, the effective rotational temperature of the 15–15 band at 407—413 nm can be estimated relatively easily, because this band is scarcely overlapped with other vibrational bands in this wavelength region. The effective rotational temperature was determined by the Boltzmann plot for the rotational lines in the R branch of the 15–15 band. The pressure dependence of the rotational temperature is shown in Fig. 1. The rotational temperature was found to decrease as the total pressure increased and approached to that at the room temperature in the high-pressure region.

Duewer et al. introduced the steady-state model for their analysis of the redistribution of the population from a specified perturbed level to other rotational lev-

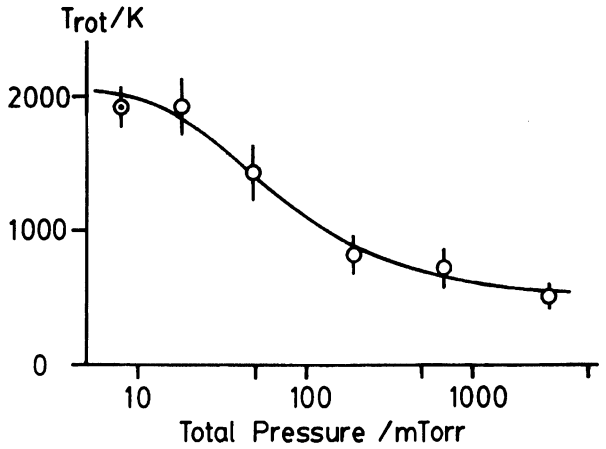

Fig. 1. Pressure dependence of the effective rotational temperature of the CN($B^2\Sigma^+$, $v=15$) state. Open circles represent the observed values and the solid curve the best-fit simulation. Error bars represent one standard deviation on the Boltzmann plot analysis. The value obtained with no additional collision partner through the second orifice is shown by a circle with a center dot (◉).

els by collisional relaxation.[3] This model can be applied to an analysis of the pressure dependence of the rotational temperature. In their analysis, the initial populations are taken as zero except for the perturbed level, because they concluded that the CN($B^2\Sigma^+$) radicals were not produced directly but formed through the perturbation from the $^4\Sigma^+$ state. However, the CN($B^2\Sigma^+$) radicals were found to be formed directly in the low-pressure experiment, as described in Ref. 7. In our analysis, the initial distribution was assumed to follow the Boltzmann distribution taken from the emission spectrum observed at the lower limit of the ambient pressure.

The above-mentioned model of ours was applied to the rotational relaxation of the B($^2\Sigma^+$, $v=15$), by which the pressure dependence of the rotational temperature was reproduced as shown in Fig. 1. The value of the cross section for collisional rotational relaxation, σ, obtained by this analysis was 95±15 Å^2, which was close to 85 Å^2 estimated at the $B^2\Sigma^+$, $v=11$ state by Duewer et al.[3]

Pressure Dependence of Intensity Anomalies in the Perturbed Lines. The pressure dependences of the intensity anomalies at (v_B, N)=(0, 15) and (11, 20) shown in Figs. 2 and 3 are due to the $B^2\Sigma^+$ ($v=0$)~$A^2\Pi_i$ ($v=10$) and $B^2\Sigma^+$ ($v=11$)~$^4\Sigma^+$ perturbations, respectively. These figures represent how the observed intensity ratio, $(I_E+I_M)/I_{env}$, depend on the ambient pressure, where I_E and I_M denote the intensities of the extra and main lines, respectively. I_{env} is the intensity of the unperturbed rotational line estimated from the envelope of the vibrational band by interpolation. Figure 2(b) shows the observed intensity ratio, I_E/I_M, for the $B^2\Sigma^+$~$A^2\Pi_i$ perturbation. For

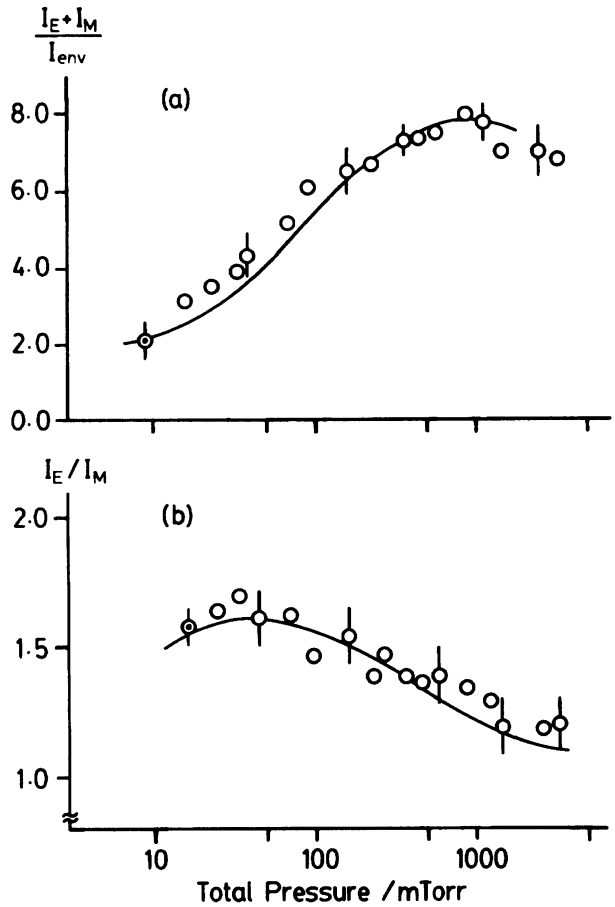

Fig. 2. Pressure dependence of the intensity ratio, (a): $(I_E+I_M)/I_{env}$, and (b) I_E/I_M, in the $B^2\Sigma^+$~$A^2\Pi_i$ perturbation. See legend of Fig. 1 for the symbols.

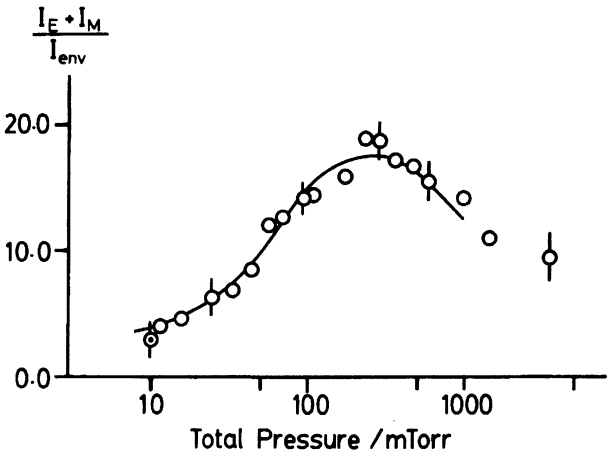

Fig. 3. Pressure dependence of the intensity ratio, $(I_E+I_M)/I_{env}$, in the $B^2\Sigma^+$~$^4\Sigma^+$ perturbation. See legend of Fig. 1 for the symbols.

the $B^2\Sigma^+$~$^4\Sigma^+$ perturbation, the main and extra lines were not resolved in our spectrum; therefore, the ratio, I_E/I_M, could not be obtained. These figures show the following features: (1) The intensities of the perturbed lines relative to that of the band envelope increase with the total pressure in the low-pressure region, whereas

they decrease in the higher-pressure region. (2) The ratio of the intensity of the extra line to that of the main line decreases with the total pressure. These features are common in the $B^2\Sigma^+\sim{}^4\Pi$ perturbation described in Ref. 8.

The observed increase in its relative intensity in the low-pressure region can be ascribed to the rotational relaxation in the long-lived perturbing state. The radiative lifetimes of $B^2\Sigma^+$ are ca. 55 and ca. 85 ns for $v=0$ and 11, respectively, and that of the $A^2\Pi_i$, $v=10$ state is reported to be ca. 5.2 μs.[11] The $^4\Sigma^+$ state is the lowest quartet state; therefore, this state can be regarded as metastable. The decrease in the relative intensity in the higher-pressure region corresponds to the rotational relaxation in the short-lived $B^2\Sigma^+$ state. On the other hand, the decrease in the intensity of the extra line relative to the main line represents the relaxation from the relatively long-lived extra state to the short-lived main state.

This treatment for the pressure dependence of the rotational temperature is not applicable in a simple manner to an analysis of the intensity anomalies in the perturbed lines, because two electronically excited states of CN with different lifetimes are coupled through perturbation. Therefore, a doorway model was set up by a modification of the steady-state model. The details of the doorway model were described in Ref. 8. In this model, collisional intraelectronic pure-rotational transitions and interelectronic transitions only at the perturbed levels are included, whereas collisional interelectronic transfer between the unperturbed levels and the collisional transitions between spin-orbit states are ignored (See Appendix in Ref. 8).

The best-fit calculated curves of the pressure dependences of the perturbed lines, $(I_E+I_M)/I_{env}$ and I_E/I_M, on the basis of this method are shown in Figs. 2 and 3. The pressure dependences of the intensity anomalies due to the $B^2\Sigma^+\sim A^2\Pi_i$ and $B^2\Sigma^+\sim{}^4\Sigma^+$ perturbations were reproduced as well as those for the $B^2\Sigma^+\sim{}^4\Pi$ perturbation system. In other words, the pressure dependences of the intensity anomalies in the rotational lines due to local perturbations can be interpreted by the "doorway" rotational relaxation model.

Rotational Relaxation of Excited CN Radicals by Collision with Rare Gas Atoms. The cross section for the rotational relaxation, σ, cannot be determined precisely from the present work because σ correlates strongly with the branching fraction and the radiative lifetime of the perturbing electronic state. The values of σ were estimated to be 50—100 Å^2 for the $B^2\Sigma^+$ and $^4\Sigma^+$ states, while that for the $A^2\Pi_i$ state was obtained to be lower than 30 Å^2.

Long-range interaction plays a significant role in collision-induced rotational relaxations.[8] The long-range interaction between the excited CN radical and the rare gas atom is mainly composed of dipole-induced dipole interaction and/or dispersion interaction, because the excited CN radical is polar and the rare gas atom is isotropic. It can be explained by the dipole-induced dipole interaction that the cross section of the $A^2\Pi_i$ state for rotational relaxation is smaller than those of the $B^2\Sigma^+$ and $^4\Sigma^+$ states.

The interaction energy of the dipole-induced dipole interaction is expressed as

$$w = -\frac{{\mu_A}^2\alpha_B}{{R_{AB}}^6} , \quad (1)$$

where μ_A is the dipole moment of the CN radical, α_B is the polarizability of the colliding rare gas atom, Rg, and R_{AB} is the distance between CN and Rg. The transition rate, k, for a fixed interparticle distance can be estimated by the Fermi golden rule[14]

$$k = 2\pi h^{-1}\rho w^2 = (2\pi/h)\rho{\mu_A}^4{\alpha_B}^2/{R_{AB}}^{12} , \quad (2)$$

where ρ is the density of states.

Equation 2 implies that the difference in the cross sections for the $B^2\Sigma^+$, $^4\Sigma^+$ states and the $A^2\Pi_i$ state is due to the difference in the dipole moment, μ_A. This can be checked if the dipole moments of these states

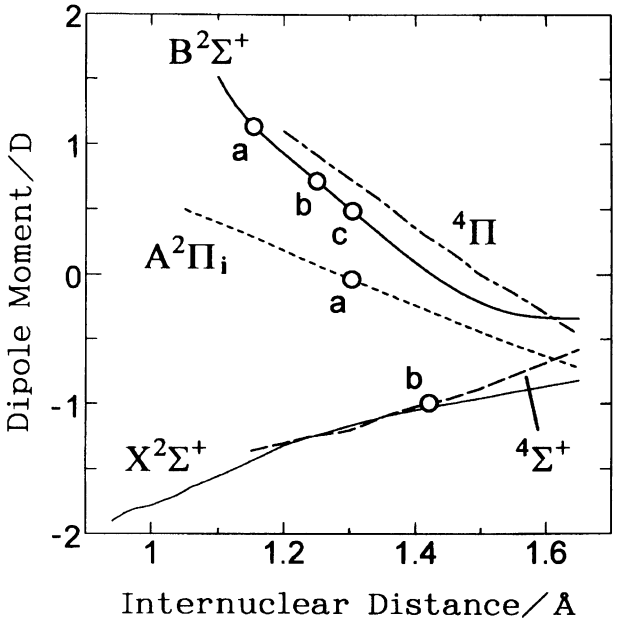

Fig. 4. Calculated electric dipole moment functions of CN. Positive sign corresponds to the polarity of C^-N^+. —— :$B^2\Sigma^+$, —— :$X^2\Sigma^+$, - - - :$A^2\Pi_i$, – – :$^4\Sigma^+$, and – – – :$^4\Pi$ states. Symbol **a** represents the dipole moments at the internuclear distances corresponding to the $B^2\Sigma^+$ ($v=0$) and $A^2\Pi_i$ ($v=10$) states, where the intensity anomalies due to the perturbation between these states are observed. Symbol **b** represents the dipole moments at the internuclear distances corresponding to the $B^2\Sigma^+$ ($v=11$) and $^4\Sigma^+$ states, where the intensity anomaly due to the perturbation between these states is observed. Symbol **c** represents the dipole moment of the $B^2\Sigma^+$ ($v=15$) state, whose effective rotational temperature was measured as a function of the ambient pressure.

are known. The dipole-moment functions for the $B^2\Sigma^+$ and $A^2\Pi_i$ states have been estimated experimentally and theoretically.[15] Nevertheless, the dipole moment of the $^4\Sigma^+$ state has not been reported. The potential energy curves of the low-lying $X^2\Sigma^+$, $A^2\Pi_i$, $B^2\Sigma^+$, $^4\Sigma^+$, and $^4\Pi$ states of CN were calculated by the MC SCF (CAS SCF) method in Ref. 16. From this calculation, the estimated dipole moment of $A^2\Pi_i$ ($v=10$), -0.05 D at $r_{C-N}=1.3$ Å, is much smaller than those of the $B^2\Sigma^+$ and $^4\Sigma^+$ states, as shown in Fig. 4. The difference in the cross sections for rotational relaxation in the excited electronic states of the CN radical is, therefore, understood in terms of that in their dipole moments.

Concluding Remarks

Strong pressure dependences of intensity anomalies in the perturbed lines and the effective rotational temperature in the CN($B^2\Sigma^+$–$X^2\Sigma^+$) emission spectra have been studied. These pressure dependences can be explained by the collision-induced rotational relaxation. The doorway model for the two-state relaxation is shown to be applicable. The state-dependent cross section for the rotational relaxation is consistent with the dipole moment calculated by the MC SCF method.

The authors are grateful to Professors K. Takatsuka, Y. Osamura, and H. Nakamura for their joint work for calculation of the dipole moment of the CN radical. The authors thank Professor S. Katsumata for his interest and encouragement in the present study. K. S. is grateful to the Toyota Physical and Chemical Research Institute for partial financial support.

References

1) H. P. Broida and S. Golden, *Can. J. Chem.*, **38**, 1666 (1960).
2) H. E. Radford and H. P. Broida, *J. Chem. Phys.*, **38**, 644 (1963).
3) W. H. Duewer, J. A. Coxon, and D. W. Setser, *J. Chem. Phys.*, **56**, 4355 (1972).
4) J. A. Coxon, D. W. Setser, and W. H. Duewer, *J. Chem. Phys.*, **58**, 2244 (1973).
5) Y. Ozaki, H. Ito, K. Suzuki, T. Kondow, and K. Kuchitsu, *Chem. Phys.*, **80**, 85 (1983).
6) H. Ito, Y. Ozaki, T. Nagata, T. Kondow, and K. Kuchitsu, *Can. J. Phys.*, **62**, 1586 (1984).
7) K. Kanda, H. Ito, K. Someda, K. Suzuki, T. Kondow, and K. Kuchitsu, *J. Phys. Chem.*, **93**, 6020 (1989).
8) K. Kanda, H. Ito, K. Suzuki, T. Kondow, and K. Kuchitsu, *Bull. Chem. Soc. Jpn.*, **65**, 481 (1992).
9) H. Beutler and M. Fred, *Phys. Rev.*, **61**, 107 (1942).
10) T. A. Miller, R. S. Freund, and R. W. Field, *J. Chem. Phys.*, **65**, 3790 (1976).
11) D. C. Cartwright and P. J. Hay, *Astrophys. J.*, **257**, 383 (1982).
12) J. I. Steinfeld, *Acc. Chem. Res.*, **3**, 313 (1979).
13) A. R. Hochstim, "Kinetic Processes in Gases and Plasmas," Academic, New York (1969), p. 419.
14) L. I. Schiff, "Quantum Mechanics," McGraw-Hill, New York (1955), p. 285.
15) R. Thomson and F. W. Dalby, *Can. J. Phys.*, **46**, 2815 (1968); S. Green, *J. Chem. Phys.*, **57**, 4694 (1972); T. J. Cook and B. H. Levy, *J. Chem. Phys.*, **59**, 2387 (1973); G. Das, T. Janis, and A. C. Wahl, *J. Chem. Phys.*, **61**, 1274 (1974); H. Lavendy, G. Gandara, and J. M. Robbe, *J. Mol. Spectrosc.*, **106**, 395 (1984); P. J. Knowles, H. -J. Werner, P. J. Hay, and D. C. Cartwright, *J. Chem. Phys.*, **89**, 7334 (1988).
16) H. Ito, Y. Ozaki, T. Nagata, T. Kondow, K. Kuchitsu, K. Takatsuka, H. Nakamura, and Y. Osamura, *Chem. Phys.*, **98**, 81 (1985).